Charged Molecular Films on Brownian Particles: Structure, Interactions, and Relation to Stability

ARTICLE *in* THE JOURNAL OF PHYSICAL CHEMISTRY B · JULY 2008

Impact Factor: 3.3 · DOI: 10.1021/jp801423h · Source: PubMed

4 AUTHORS, INCLUDING:

Alessio Zaccone
University of Cambridge
65 PUBLICATIONS **501** CITATIONS

SEE PROFILE

Charged Molecular Films on Brownian Particles: Structure, Interactions, and Relation to Stability

Alessio Zaccone, Hua Wu, Marco Lattuada, and Massimo Morbidelli*

Institute for Chemical and Bioengineering, Department of Chemistry and Applied Biosciences, ETH Zurich, 8093 Zurich, Switzerland

Received: February 18, 2008; Revised Manuscript Received: March 13, 2008

The interfacial film of physically adsorbed ionic amphiphilic molecules on submicron particles dispersed in water was studied by a combination of surface tension measurements, laser light scattering (LLS) and high-shear experiments in a microchannel. General features in the structure and morphology of the molecular film are identified and understood in the framework of the two-step Langmuir adsorption model deduced from the adsorption isotherm. On the basis of this approach, the phase transitions and structural ordering of the film at the solid−liquid interface are analyzed in detail. A novel methodology based on high-shear aggregation experiments subsequently analyzed by means of LLS is proposed and turns out to be able to provide significant information on the phase transitions and structural arrangements of the adsorbed molecules (in substantial agreement with the adsorption isotherm model) as well as on the resulting interactions. Particularly important for applications is the result that, with no added salt, the films on two particles can adhere/fuse, leading to aggregation as long as an uncovered (hydrophobic) patch is present (unsaturated molecular layers). In the opposite case of fully developed layers, by analyzing the mechanism of shear aggregation of charged particles in the low-salt limit, we show that, when the hydrophobic attraction is absent, short-range hydration repulsive forces dominate over Derjaguin−Landau−Verwey−Overbeek (DLVO) forces and adhesion can never be achieved even upon application of very high collision energies. Consistently, a lower limiting boundary for the hydration interaction is calculated and found to be in agreement with data in the literature.

I. Introduction

Understanding the surface properties of nano and submicron particles for better control over their interactions, stability and functionalization is currently a key issue in nano- and bionanotechnology. In most cases, the interface of the nanoparticles is represented by a shell of self-assembled organic molecules or macromolecules.[1] Furthermore, charged organic molecules adsorbed on the surface are ubiquitous in such systems, and their morphology and assembly are of fundamental importance for the functionalization, recognition, and selectivity of the particles surface in relation to physiological and therapeutic issues.[2–4] The interactions of such shells are a critical point in designing tailored particles for drug delivery since they affect fundamental parameters such as retention times, modality of release, and attachment onto the target. Therefore, fundamental understanding of the interactions of such particles is necessary. However, despite intense studies in surface science over the past decades, satisfactory knowledge about the structure and interactions of organic molecular layers on nanoparticles is still lacking. Considerable progress has been achieved in characterizing flat surfaces by means of a variety of techniques, including neutron reflection techniques, atomic force microscopy (AFM) and the surface force apparatus.[5–7] The latter two techniques have been crucial to the understanding of the structure of surfactant molecules on flat substrates,[8] and an improved version of AFM has been recently used to resolve adsorbed layers of surfactants with unprecedented detail, even on rough surfaces.[9] Interesting results have also been obtained by means of Rutherford backscattering on latex films covered with surfactant.[10] The interface of nanoparticles, in comparison with flat surfaces, is by far less accessible because of the intense Brownian motion of submicron particles in a liquid. In some cases, the surface of the nanoparticles is assumed to be equal to that of a substrate made of the same material, but this assumption is very strong since it is well-known that the surface of nanoparticles shows profound differences with respect to that of mesoscopic substrates of the same material.[11] Attempts to apply AFM to nanoparticles have been made by Drelich et al.[12] by electrostatic deposition of charged nanoparticles on a substrate. However, considerable obstacles toward the resolution of the probe−nanoparticle interaction are given by the lack of knowledge about the layering and structure of the deposited particles as well as about the superposed interaction with the substrate. Thus, the only reliable experimental techniques still seem to be the scattering of radiation and, in order to study adsorbed molecules, the traditional adsorption isotherm based on analysis of the depleted solution.[13,14] Pioneering work done by Wu[15,16] in the 1990s has given insight into the interface of latex nanoparticles polymerized with surfactants by using LLS within the Rayleigh−Debye−Gans (RDG) limit. Adsorption of surfactant molecules on colloidal particles has been studied extensively in the past by means of neutron scattering and dynamic light scattering (DLS) combined with adsorption isotherms.[17,18] In the latter case, the DLS measurements are intrinsically affected by the uncertainty in the position of the shear-plane around the particles, which might lead to an overestimation of the adsorbed layer.[18] In our previous work, we proposed a technique based on a combination of static light scattering and scanning electron microscopy that, by using the Lorenz-Mie theory, enables the resolution, down to the nano-

* Corresponding author. E-mail: morbidelli@chem.ethz.ch.. Fax: 0041-44-6321082.

10.1021/jp801423h CCC: $40.75
Published on Web 05/13/2008

scale, of the molecular layer's height on the surface of particles of any size within the colloidal domain.[19] Structural information could thus be extracted about the orientation and conformation of the adsorbed molecules as a function of the surfactant amount present in the system. Although this provides an independent experimental support to the two-step Langmuir theory for van der Waals adsorption of amphiphilic molecules, further insight into the interaction of the molecular shells is needed in order to understand and predict the behavior with respect to stability and adhesion of this important class of nanoparticles.

In this work, we present a new approach to probe the structure and interactions of charged molecular films adsorbed on submicron Brownian particles. In the first part, we characterize the films formed by two different anionic surfactants on polymer particles by means of the well-established adsorption isotherm-based method. On applying the two-step Langmuir model, structural information is obtained about the different phases of the 2D molecular domains encountered with increasing surfactant concentration. The scenario inferred, however, relies uniquely on one experimental technique, namely, the adsorption isotherm constructed by measuring the surface tension of the depleted solutions. In order to have a more robust validation of this theory as well as information on the interactions, the dispersions are sheared in a microchannel (MC) at a very high shear-rate. The extent of particle−particle aggregation at varying surfactant concentration, as measured by laser light scattering (LLS), is then related to the structural phases in the corresponding regimes of concentration. This is done in the absence of added electrolyte so as to better resolve the interparticle interaction and to avoid undistinguished massive coagulation of the particles across the whole surfactant concentration range. A correlation between the structural phases predicted by the adsorption theory and the different aggregation regimes is sought. The surface-mediated interparticle interactions involved were investigated by means of mean-field calculations based on the Derjaguin−Landau−Verwey−Overbeek (DLVO) theory combined with a simple model for the energy of particle−particle collision in the applied flow field. The question of how to interpret this data about interactions was then answered within the framework developed by Israelachvili and co-workers for surfactant and lipid bilayers.

II. Experiments and Methodology

The Colloidal System and Sample Preparation. We used a colloidal dispersion constituted by styrene−acrylate copolymer latex supplied by BASF AG (Ludwigshafen, Germany), produced by emulsion polymerization. The particles, with a mean radius of $R_p = 289$ nm, have been described in our previous paper.[19]

Two different surfactants, an aliphatic C-18 carboxylate (denoted by C) and an aliphatic C-15 sulfonate (denoted by S) surfactant, respectively, have been used in this study. For the former, its association phenomena and interaction with the particles surface have already been studied extensively and described in our previous work.[19]

It was necessary to remove the surfactant used for the polymerization process from the latex as well as the residual initiator and other impurities before the surfactant adsorption experiments. This has been done by mixing the latex with a mixture of cationic and anionic ion-exchange resins (Dowex MR-3, Sigma-Aldrich), according to a procedure that has been described elsewhere.[19] The water used for dilution was Milli-Q water in all cases. All the experiments have been carried out in the low-salt limit, with no added electrolyte. In the C system, because of the slightly basic character of the surfactant itself, the pH value is always found to be around 8.

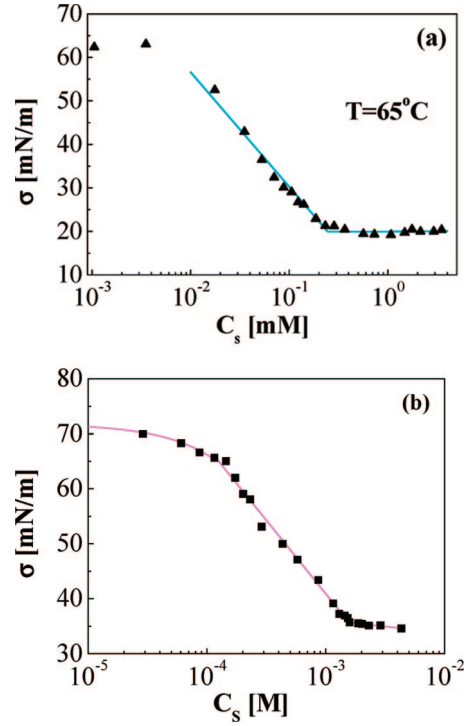

Figure 1. Surface tension (calibration) curves for the C (a) and the S (b) surfactants. Note that the curve for the C surfactant was measured at $T = 65$ °C, owing to the low solubility of C at room temperature. The calibration curve for S was measured at $T = 25$ °C.

Adsorption Isotherm Measured by Surface Tension and Theoretical Methods. Surface tension measurements have been employed to obtain the adsorption isotherm of the amphiphilic molecules on the particles. The adsorption experiments were carried out at 25 °C for all samples following the procedure described in our previous paper.[19] After centrifugation of the particles, the surface tension of the supernatant depleted of particles was analyzed by means of the Wilhelmy plate method using a DCAT-21 tensiometer (Dataphysics, Germany). It is known that the solubility of the C surfactant at room temperature is low. In order to avoid its precipitation, we obtained the calibration curve relative to pure C in water at 65 °C. The calibration curve of S was obtained at 25 °C. The two curves are shown in Figure 1, and the sharp knee indicating the transition to the micellar regime, in both cases, reveals excellent purity grade of the material.

Similar to those of most systems involving the adsorption of amphiphilic molecules on hydrophobic substrates in aqueous environment, the experimental adsorption isotherm has been fitted with good agreement by means of the theoretical model known as the "L−S" or "two-step" adsorption isotherm, originally developed by Zhu and Gu.[20] The model is derived on the basis of a thermodynamic equilibrium treatment analogous to that used by Langmuir, i.e., considering the reactions between free sites at the particle surface and the surfactant molecules. In this case, a first step is assumed where the molecules adsorb one by one, and they adopt an extended conformation aligned with the surface in order to maximize the hydrophobic attractive interaction with the substrate. A second step follows where the previously adsorbed single molecules anchor bunches of $n - 1$ molecules to form condensed assemblies of n molecules (also referred to as "hemimicelles")

where the molecules interact via van der Waals forces. This second step is linked with a considerable increase in the adsorption density. The mathematical form of the L−S adsorption isotherm is as follows:[20]

$$\Gamma = \frac{\Gamma_\infty k_1 C\left(n^{-1} + k_2 C^{n-1}\right)}{1 + k_1 C\left(1 + k_2 C^{n-1}\right)} \quad (1)$$

where C is the bulk surfactant equilibrium concentration, k_1 and k_2 are the equilibrium constants for the two adsorption steps, and Γ and Γ_∞ are the equilibrium and the saturation adsorption densities at the surface, respectively. Note that the parameter n should be most conveniently interpreted as the mean number of monomer molecules interacting via van der Waals forces. Since the van der Waals forces are typically short-ranged, values of n much larger than 10 are rarely found. Condensed nuclei of, on average, n molecules, thus have to be regarded as the building blocks of the condensed domains. This simple equation contains all the basic conceptual tools that have been hitherto used in the analysis of the structural phases and transitions involving amphiphilic molecules adsorbed on hydrophobic substrates. On the basis of its derivation, the equilibrium constants for the two reaction steps are given by $k_1 = (\Gamma_1/\Gamma_F)C$ and $k_2 = (\Gamma_K/\Gamma_1)C^{n-1}$, respectively. The quantities Γ_F, Γ_1, and Γ_K, are the surface densities of free sites, adsorbed monomers, and condensed domains, respectively. Note that the site densities, Γ_F, Γ_1, and Γ_K, are hemimicelle-based. It is clear that $\Gamma = \Gamma_1 + n\Gamma_K$ and $\Gamma_\infty = n(\Gamma_F + \Gamma_1 + \Gamma_K)$. Combining all these relations, it is possible to derive single adsorption isotherms for the unoccupied sites, the monomers, and the condensed phase, respectively:

$$\theta_F \equiv \frac{\Gamma_F}{\Gamma_\infty/n} = \frac{1}{1 + k_1 C + k_1 k_2 C^n} \quad (2)$$

$$\theta_1 \equiv \frac{\Gamma_1}{\Gamma_\infty/n} = \frac{k_1 C}{1 + k_1 C + k_1 k_2 C^n} \quad (3)$$

$$\theta_K \equiv \frac{\Gamma_K}{\Gamma_\infty/n} = \frac{k_1 k_2 C^n}{1 + k_1 C + k_1 k_2 C^n} \quad (4)$$

The above relations, built upon the experimental knowledge of the adsorption parameters, provide insight into the structure and evolution of the adsorbed film as a function of the surfactant concentration in the system. From a thermodynamic point of view, the spreading pressure of the film is defined in analogy with the pressure of a 3D vapor with the volume V being replaced by the area A: $\pi \equiv -(\partial F/\partial A)_{T,V}$, where F is the total free energy of the system. Extending results from the thermodynamics of ordinary solutions,[24] the following inequalities apply: $(\partial\mu/\partial\Gamma)_T > 0$, where μ is the chemical potential of the adsorbate, and from the Gibbs−Duhem relation: $\Gamma = -(\partial\sigma/\partial\mu)_T = -(\partial\sigma/\partial\Gamma)_T(\partial\Gamma/\partial\mu)_T$. The latter one implies that $(\partial\sigma/\partial\Gamma)_T < 0$. Since $(\partial\pi/\partial\mu)_T = \Gamma > 0$, it is clear that $(\partial\pi/\partial\Gamma)_T > 0$, as well. This means that $d\pi = -d\sigma$. The latter result can be inserted into the Gibbs relation ($\Gamma = -[C/(RT)](d\sigma/dC)$) yielding the well-known result $\pi = RT\int_C^0 \Gamma d(\ln C)$, which directly correlates the spreading pressure with the adsorption isotherm. Integration of the analytical expression (eq 1) was carried out by Zhu and Gu[21] and leads to the following relation, which gives π as a function of the adsorption parameters and the equilibrium concentration:

$$\pi = (\Gamma_\infty/n)RT\ln\left(1 + k_1 C + k_1 k_2 C^n\right) \quad (5)$$

When the theoretical fit is of good quality, application of (eq 5) allows the determination of π, thus avoiding the singularity that would arise upon graphical integration of the experimental curve in the limit $C \to 0$, $\ln C \to -\infty$.

The spreading pressure π is an important physical parameter, and the curve of π versus A (the effective area occupied by a surfactant molecule at the surface) that can be constructed by means of (eq 5) is a fundamental tool to study the structure and phases of films on surfaces. It is such curves that clearly indicate the transition between phases and their equilibria. In the following, we will refer to two main states or phases of the molecules: the gaseous state (G), corresponding to individually adsorbed molecules, and the condensed state (K). The gaseous state corresponds to noninteracting individually adsorbed molecules, of which the spatial arrangement on the surface does not possess any degree of order, while the condensed state, which in the past has been imprecisely defined as "crystalline", is more likely a state where degrees of order higher than short-range (also known as "extended" short-range order) are present. In 1D and 2D atomic or molecular arrays, no long-range order can be there at temperatures above the absolute zero, as demonstrated by Peierls and Landau, respectively.[22,23] Since the mean squared displacement in the position of the atoms/molecules diverges logarithmically, however, limited quasi-crystalline domains smoothed out by the thermal fluctuations can exist[24,25] (it is furthermore recognized, now, that higher degrees of order quantifiable by an order-metrics approach can be present in hard-sphere and van der Waals systems traditionally identified as liquid-like[26]).

The Shearing Device and Laser Light Scattering. It is a well-established approach, in chemical physics, to apply high pressure differences and intense flows with the aim to draw information about inter- and intramolecular interactions in molecular complexes. The most common approach is to use slit-jet (supersonic) nozzles where, as a consequence of the high-pressure difference expansion, the aggregation and decomposition of molecules is induced in order to shed light on the interactions. The changes in the association, decomposition, as well as the conformational modifications produced in the nozzle are then analyzed by means of various spectroscopic techniques. We thus applied this general strategy to the case of Brownian particles, for which, in contrast to non-Brownian and supramicron particles, other probing methods are inapplicable. Following the procedure reported in our previous work[19] and using the devices therein described, we applied an intense flow field to the dispersion by imposing a pressure drop of about 83 bar across an MC, which results in an average shear-rate $\dot{\gamma} = 8.15 \times 10^5\ s^{-1}$. Inside the MC, the highest shear-rate (linked with the turbulent velocity gradients) is localized near the wall of the MC. Thus, a curvilinear MC has been constructed in order to enhance the mixing and the residence time so as to guarantee the transit of the sample throughout the whole cross-section of the channel. More details about the characterization of the flow-field inside the MC can be found in our previous contribution.[19] The spectroscopic analysis in the present case is carried out ex situ on the sheared dispersion sampled at the outlet of the MC, and, upon dilution to avoid multiple scattering, the aggregates formed are measured by a small-angle light scattering (SALS) instrument. The average radius of gyration, $\langle R_g \rangle$, of the aggregates is thus determined in the well-known Guinier approximation regime.

The SALS instrument used to quantify the extent of aggregation inside the MC is the Mastersizer 2000 (Malvern, U.K.), with a scattering angle range from 0.02° to 40° and a laser beam wavelength of $\lambda_0 = 633$ nm. A more detailed description of the instrument can be found elsewhere.[27]

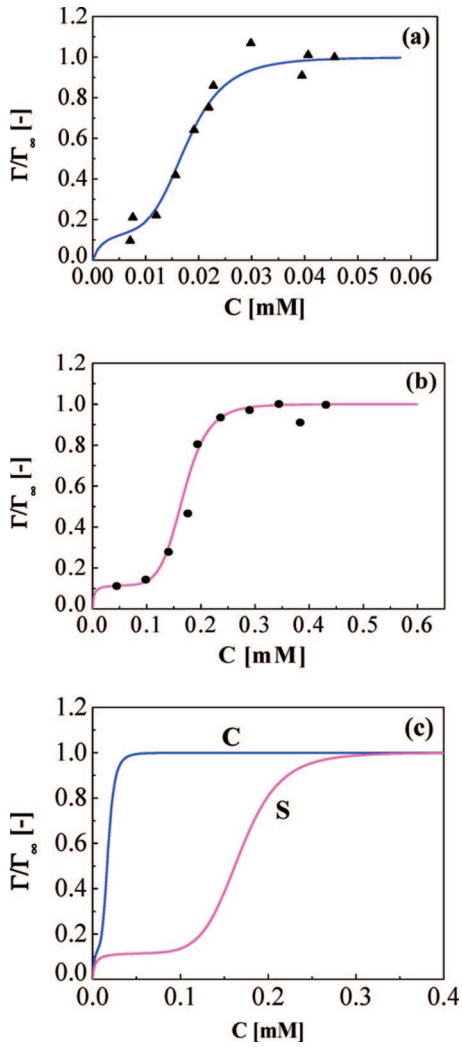

Figure 2. Adsorption isotherms for the C (a) and the S (b) surfactant, as measured at $T = 25$ °C by means of the surface tension technique on the solution depleted of particles. Symbols: experimental data. Continuous lines: fitting obtained by means of eq 1. Values of the fitting parameters are given in Table 1. The theoretical fitting curves are plotted in panel c for comparison.

TABLE 1: Adsorption Parameters, Molecular Area at Saturation, and Gibbs Free Energy of Association for the Two Surfactant Systems, Carboxylate (C) and Sulfonate (S)

surfactant	k_1	k_2	n	A_m (Å^2)	ΔG_K^0 (kJ mol^{-1})
C	1.44×10^5	1.6×10^{20}	5.73	26	−20116
S	4×10^5	5×10^{27}	8.35	72	−18925

III. Results and Discussion

The Adsorption Isotherms. Figure 2a,b shows isotherms of adsorption for the C and S surfactant systems on the styrene−acrylate copolymer particles, respectively. The fitting given by eq 1 is good in both cases. The adsorption parameters found from the fitting are summarized in Table 1 with the respective Gibbs free energy of condensation (or hemimicellization) calculated from $\Delta G_K^0 = -(1/n)RT \ln k_2$, with R being the ideal gas constant.[28] Comparing the two fitting curves in Figure 2c, it is evident that, in the case of the C surfactant, the whole adsorption isotherm is shifted to much lower equilibrium concentrations, which is expected given the highly hydrophobic character of the C-18 molecule. Therefore, also the association−condensation phenomena at the surface set in at a much lower concentration for the C surfactant than for the S surfactant, which has a shorter hydrophobic tail. The obtained two values for the Gibbs free energy relative to the associative step of the surfactant molecules in Table 1 are in rather good agreement with typical values for the second step of adsorption of surfactants on hydrophobic substrates.[28] As in any molecular assembly process, the association of the molecules occurs as a competition between a favorable enthalpic term due to the formation of noncovalent (mainly van der Waals) bonds and the unfavorable entropic term due to the intrinsic loss of (mainly) translational entropy involved in the assembly.[29] The difference in the Gibbs free energy of condensation for the two systems can be explained by the fact that the favorable enthalpic term is directly proportional to the surface of contact involved in the noncovalent bond, which is clearly larger for molecules having longer chains, as in the case of the C molecule. Furthermore, the entropically favored breaking of highly structured water in contact with the hydrophobic chains also contributes to the enthalpic term (hydrophobic interaction), and this contribution becomes of course more important with longer hydrophobic chains, as in the case of the C molecule. The area occupied by a surfactant molecule at the surface at saturation is calculated from $A_m = 1/(\Gamma_\infty N_A)$, where N_A is Avogadro's number. The resulting values are reported in Table 1 and are 26 Å^2 and 72 Å^2 for the C and S systems, respectively. The two values are quite different. One reason for this resides, once more, in the different chain length. It is well-known that longer chains occupy a smaller area in the saturated monolayer as a result of the decreased mobility brought about by the stronger attractive association forces. This is why, as noted already in our previous work, the value 26 Å^2 for the C system is close to that measured in close-packed bilayers of the same surfactant by X-ray diffraction.[31] The second reason for this difference rises from the fact that only about 20% of the C molecules (at pH = 8) are dissociated, while the S molecules are dissociated to a much higher extent. Thus, the unscreened electrostatic repulsion, with no added salt, is much stronger in the case of the S surfactant and leads to larger intermolecular spacing at saturation.

On the basis of eqs 2–4, single adsorption isotherms for the free sites, the adsorbed monomers and the condensed phase have been calculated for the two systems. They are plotted in Figure 3a,b as a function of the equilibrium concentration of the surfactant. It is seen that, in the range of low surface coverage, the fraction of free sites (θ_F) decays more rapidly for the S than for the C surfactant. The adsorption of single molecules, in the corresponding regime, is sensibly higher, and reaches higher values in the case of the S molecule, as reflected in the trend of θ_1 (which is the fraction of adsorbed single molecules in the G phase). Practically, as a consequence of the more negative ΔG_K^0 of C compared with S, as explained above, the associative step of adsorption in the case of C starts at concentrations where patches of free particle surface are still present. This means that, in the range $C \approx 0.01-0.02$ mM, three phases (namely, the G, the K, and the free particle surface) coexist in the case of the C surfactant. In the case of the S surfactant, however, when the K phase is present, the free particle surface vanishes.

The Spreading Pressure. Further insight, especially into the structure and transitions of the adsorbed phases, can be derived from the $\pi-A$ curves constructed on the theoretical fit by means of eq 5. These are shown in Figure 4a. It is immediately evident that the two curves, for C and S, are quite different. The $\pi-A$ curve for the C surfactant is rather complex. The spreading pressure increases gradually with the concentration, and a short

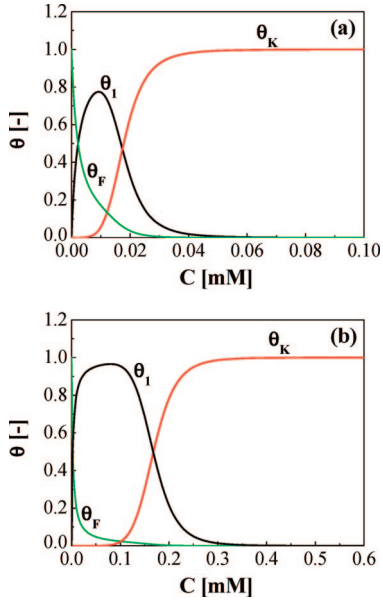

Figure 3. Individual adsorption isotherms (individual fractional coverages as defined according to eqs 2–4) plotted as a function of the bulk equilibrium concentration of surfactant: (a) C system; (b) S system. The meaning of the curves is explained in the text.

intermediate regime is then encountered prior to the transition to the asymptotic behavior upon approaching the saturation limit. On the basis of the single adsorption isotherm, one might expect a coexistence region between gas and condensed phases for the C system. The coexistence region between two phases at equilibrium usually appears in the form of a plateau in the $\pi-A$ curve (also in analogy with the $P-V$ curves of 3D systems). In Figure 4b the $\pi-A$ curve of the C surfactant is plotted together with the single isotherm curves, as a function of the degree of coverage, Γ/Γ_∞. It is evident that the narrow intermediate region between G and K phases in the $\pi-A$ curve starts when θ_K becomes significant while θ_I starts decreasing. However, the expected plateau of coexistence of G and K phases at equilibrium is not observed. This is because the fraction of free sites, θ_F, remains significant up to coverage values $\Gamma/\Gamma_\infty \approx 0.7$, thus preventing the two-phase coexistence equilibrium between G and K.

Different is the case of the S surfactant. Here, a plateau is clearly identified, where the G and K phases coexist at equilibrium (Figure 4b). This is because, in contrast to the C case, at the sharp turnover point at which θ_I starts decreasing while θ_K rises, θ_F is very small and becomes rapidly negligible, thus leaving a two-phase equilibrium coexistence system composed practically of K and G domains only.

We also see that, in the low coverage regime, the fraction of free sites is larger in the C system than the S case, this being also reflected in the spreading pressure of surfactant C being significantly lower than the spreading pressure of S (Figure 4a).

The schematic representation of the G phase and of the coexistence between G and K phases is reported in Figure 5. One can note that, from the model proposed in Figure 5, the conformation of the molecules changes from the G to the K phase, in that it is horizontal and aligned with the surface in the G phase while it is more vertical in the K phase. This is consistent with the two-step adsorption theory[20,33] and with our experimental results on the height of the adsorbed film as a function of the surfactant concentration obtained by light scattering and reported in our previous work.[19] Finally, the

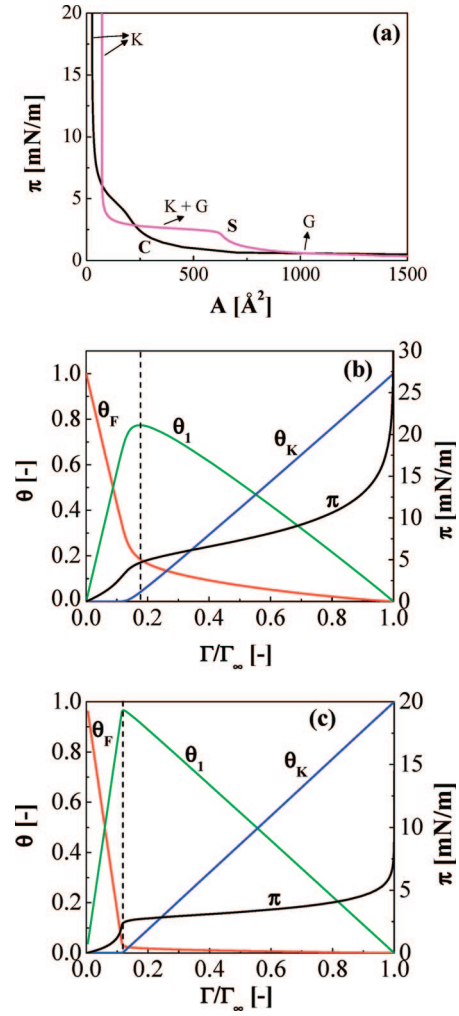

Figure 4. Spreading pressure ($\pi-A$) curves calculated with the fitted adsorption parameters according to eq 5. (a) C and S refer to the C and S surfactant systems, respectively. The meaning of the curves is explained in the text. (b,c) The spreading pressure π is plotted for the C and S system, respectively, together with the respective single adsorption isotherms as a function of the degree of coverage, Γ/Γ_∞.

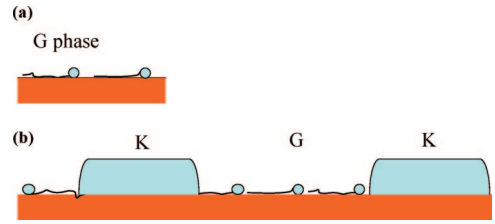

Figure 5. Schematic representation of the structure of the gaseous (G) phase, (a), and of the coexistence of gaseous (G) and condensed (K) patches, (b).

molecular areas extrapolated at the asymptotes are 26 and 72 Å^2 for the C and S system, respectively, in agreement with the values evaluated before.

Surfactant Surface Structure Probed by High Shear Rate-Induced Collisions. Figure 6 summarizes the results for the extent of high-shear aggregation induced in the MC as measured by SALS. The radius of gyration, R_g, is reported for both systems as a function of the degree of coverage, Γ/Γ_∞ in Figure 6a. Three regimes can be identified. Regime 1 at low coverage is characterized, for both C and S systems, by a considerable extent of aggregation, meaning that the collision energy imparted

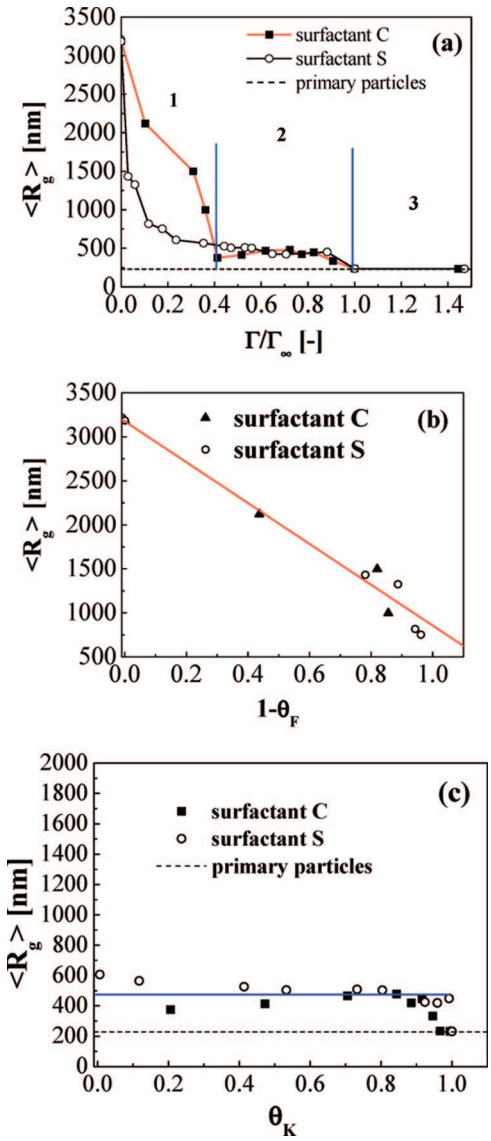

Figure 6. (a) The radius of gyration ($\langle R_g \rangle$) of the aggregates formed by shearing the dispersion in the MC as a function of the degree of coverage, Γ/Γ_∞. (b)The radius of gyration ($\langle R_g \rangle$) of the aggregates formed in regime 1 as a function of the total degree of coverage of the surface (the latter is equal to $1 - \theta_F$). (c) The $\langle R_g \rangle$ values relative to regime 2 as a function of the fractional coverage of K domains.

by the flow field is able to overcome the repulsive energy existing between the particles. This is indeed reflected in a monotonic decrease of the radius of gyration of the aggregates with the coverage. At higher values of coverage, regime 2 sets in, which is characterized by a much weaker dependence of the extent of aggregation, quantified by $\langle R_g \rangle$, upon the coverage. Practically, accounting for certain scattering in the experimental data, the extent of aggregation does not change significantly with increasing Γ/Γ_∞. Finally, regime 3 appears when the surface of the particles becomes completely covered with a fully developed monolayer of molecules and aggregation is suppressed ($\langle R_g \rangle$ coincides indeed with the radius of gyration of the primary particles). These three regimes can be understood based on the results discussed above on the structure and phases of the surfactant film on the particles. Within regime 1 the particles can aggregate because the surface is either free of surfactant or covered by gas-like domains (the latter as schematized in Figure 5a), which means that the entire surface is essentially hydrophobic and the repulsive interaction stabilizing the particles arises mainly from the charges of the individually adsorbed molecules and the original charges of the particles. The monotonic decrease of R_g can be understood by considering how the interaction energy of the particles varies with the surface charge density, through the DLVO theory. The general relation between the potential and the surface charge density for a sphere charged at the interface is given by $-\varepsilon \nabla\psi \cdot \mathbf{n} = q$, where ε is the relative dielectric permittivity of the medium, ψ is the electric potential, and q is the surface charge density. Under the assumptions of the Gouy−Chapman model,[34] in the presence of monovalent counterions, the following relation between the surface potential ψ_0 and q applies: $\psi_0 = 2kT/e_1 \sinh^{-1}[q/(8\varepsilon kT[K^+])^{-1/2}]$, where e_1 is the elementary charge, $[K^+]$ is the counterion concentration in moles per liter, and k is Boltzmann's constant. The surface potential is thus a monotonic increasing function of the surface charge density. If one calculates the electrostatic repulsive interaction using the analytical Sader−Carnie−Chan formulas,[35] including the van der Waals attractive interaction of the usual form,[36] the resulting height of the repulsive barrier is also monotonic with the surface charge density and roughly linear in the regime of moderate to high surface potentials. This leads us to infer that the "classic" DLVO repulsion, being a monotonically decreasing function of the surface coverage, is responsible for the monotonically decreasing trend in regime 1. Regarding the considerable difference in absolute values between the two systems in regime 1, we note that $\langle R_g \rangle$ is always greater for the C system than for the S system. This is due to the fact that, as shown in Figure 4b,c, within the first regime, the surface covered with the G phase increases more rapidly with the concentration for the S surfactant than for the C surfactant. The latter one, in the first regime, indeed retains a significant extent of surface that is free of molecules, as we have seen before by discussing the single isotherms and the $\pi-A$ curves (Figure 4a−c).

Regime 2 sets in with the almost complete coverage of the surface by the gas-like film accompanied by the appearance of the condensed domains. The transition to regime 2 occurs at a lower concentration for the S surfactant than for the C surfactant. This is due to the fact that since the molecular area is larger for the S surfactant than for the C surfactant, at the same total concentration, the C system still retains a significant amount of the free surface sites, while the S system is almost fully covered by the gaseous phase. With the coexistence of G and K phases (as schematized in Figure 5b), aggregation is still possible on the G patches where, as mentioned previously, the attractive hydrophobic interaction is dominant. However, since the particles are presumably able to rotate and to adjust their relative position during the aggregation process so as to aggregate on the hydrophobic patches, the efficiency of collision in the coexistence region is expected to depend very weakly, if not being independent at all, on the coverage. This is indeed what we observe in regime 2 where $\langle R_g \rangle$ is practically independent of the surface coverage, within the experimental scattering.

A rapid transition to regime 3, where no aggregation is observed, occurs when the coverage approaches the values corresponding to the saturation for the two systems, i.e., $\Gamma/\Gamma_\infty = 1$ (the transition is shifted to a higher concentration value of concentration for the S system because of the different partitioning between surface and bulk for the two systems), and aggregation is suppressed as soon as the monolayer is fully developed on the whole surface of the particles (a result that was anticipated in our previous work).[19]

In order to verify that this interpretation of the mechanisms and different interaction regimes encountered by varying the

surfactant concentration/coverage of the system is indeed of general validity and independent of the particular amphiphilic system, we have plotted the $\langle R_g \rangle$ values as a function of the relevant quantities for the first two regimes. In regime 1, the relevant quantity is the fraction of the surface that is progressively covered by the molecules. Thus, the radius of gyration for the two systems in regime 1 is plotted as a function of $1 - \theta_F$ in Figure 6b. It is seen that all the experimental data in this regime for the C and S systems collapse onto one curve and decay almost linearly with $1 - \theta_F$. This supports the explanation given above grounded on the approximately linear increase of the electric double layer (EDL) repulsive barrier with concentration/coverage. Concerning regime 2, $\langle R_g \rangle$ has been plotted in Figure 6c as a function of the fraction of surface occupied by the condensed domains θ_K. Also in this case, the two curves collapse onto one curve, which shows no dependence on the fraction of the K phase. This indicates that the probability of aggregation is the same as long as G-phase patches are still present on the surface of the particles, as discussed previously. For both cases, when the surface becomes saturated with a condensed monolayer, aggregation is no longer possible.

Stability under Shear and Interactions of Charged Particles Bearing Charged Molecular Films. In order to answer the question of why even at such high collision energy it is not possible to aggregate Brownian particles bearing a fully developed monolayer of charged amphiphilic molecules, we have performed some calculations to analyze and compare the different contributions of the interaction energies involved in the collision of two such interacting particles. The seminal work of Fuchs,[37] extending the Smoluchowski theory[38] of fast coagulation of particles to the case where interparticle interactions are accounted for, has led to the definition of a parameter, the Fuchs stability ratio W, which uses DLVO results to quantify the effects of interactions on the aggregation rate of spherical particles. However, whenever shear forces are present, the evaluation of particle stability is much more difficult, and even simple criteria are not available in the literature. In addition, most of the experimental work on aggregation in the presence of shear has been carried out in conditions of fully destabilized particles.

We hereby propose a semiquantitative criterion for the stability of particles in the presence of both shear forces and DLVO interactions, together with an estimate of theirs coagulation rate. We start from the same configuration used by both Smoluchowski and Fuchs, who considered a reference particle located at the center of a system of coordinates, and compute the flux of particles diffusing toward it. Compared to the generalized diffusion equation used by Fuchs, we have included an additional convective contribution due to the convective flux of particles dragged along by the fluid. The same approach has been used by other authors in the literature (e.g., the work of Melis et al.[39]). However, when a realistic flow field pattern is used, such as simple shear or elongational flow, the equation becomes a partial differential equation, the solution of which can only be obtained with numerical methods and is numerically very stiff when the contribution of convection is strong. We therefore assume that the flow field is generated by a sink located at the center of the reference particle. This implies that all streamlines are converging to the center of the reference particle, and the system configuration retains its spherical symmetry. In order to fulfill the continuity equation, the velocity field has to have the form

$$\mathbf{v} = -\upsilon_0 \frac{2R_p}{r^2}\mathbf{e_r} \tag{6}$$

where $\mathbf{e_r}$ is the unit vector in the radial direction, pointing outward from the reference particle, υ_0 is the relative particle velocity at the collision surface (which is the sphere having a radius equal to twice the radius of a particle R_p), and r is the distance measured from the center of the reference particle. The diffusion-convection equation for a system with spherical symmetry reads

$$\frac{1}{r^2}\frac{\partial}{\partial r}\left[r^2\left(D\frac{\partial C_p}{\partial r} + \frac{D}{kT}\frac{\partial \Phi}{\partial r}C_p + \upsilon_0\frac{4R_p^2}{r^2}C_p\right)\right] = 0 \tag{7}$$

where D is the particles relative diffusion coefficient (given by the Stokes−Einstein equation: $D = kT/3\pi\eta R_p$), η is the fluid viscosity, k is Boltzmann's constant, T is the absolute temperature, Φ is the total interaction potential energy, and C_p is the particle concentration. Equation 7 has to be solved together with the boundary conditions

$$\begin{cases} r = 2R_p \Rightarrow C_p = 0 \\ r \to \infty \Rightarrow C_p = C_{p,0} \end{cases} \tag{8}$$

The first condition establishes that, when two particles touch, aggregation ensues as a result of strong van der Waals interactions, while the second condition implies that at infinite distance from the reference particle the concentration of particles equals the bulk concentration $C_{p,0}$. Equation 7 can be solved analytically, leading to

$$\frac{C_p}{C_{p,0}} = \exp\left(\mathrm{Pe}\frac{R_p}{r} - \frac{\Phi(r)}{kT}\right)\frac{\int_{2R_p}^{r}\frac{\exp\left(-\mathrm{Pe}\frac{R_p}{r} + \frac{\Phi(r)}{kT}\right)}{r^2}\,dr}{\int_{2R_p}^{\infty}\frac{\exp\left(-\mathrm{Pe}\frac{R_p}{r} + \frac{\Phi(r)}{kT}\right)}{r^2}\,dr} \tag{9}$$

where Pe is the Peclet number, i.e., the ratio between convective and diffusive transport, defined as $\mathrm{Pe} = (12\pi\eta\upsilon_0 R_p^2)/(kT)$.

From the above solution, it is straightforward to compute the total flux of particles toward the reference particle and the corresponding aggregation rate constant:

$$K_{11} = \frac{8\pi D R_p}{2R_p\int_{2R_p}^{\infty}\frac{\exp\left(-\mathrm{Pe}\frac{R_p}{r} + \frac{\Phi(r)}{kT}\right)}{r^2}\,dr} \tag{10}$$

Equation 10 is very helpful, since it not only provides the aggregation rate constant, but also allows us to derive a useful stability criterion. First of all, in the case where no convection (no shear) is present (Pe = 0), eq 10 provides the well-known result obtained by Fuchs, and the denominator reduces to the Fuchs stability ratio W. In the case where no interactions are present and aggregation is only due to shear and diffusion, the value of the Peclet number determines the relative importance between shear and diffusion. In this case, eq 10 reduces to

$$K_{11} = \frac{8\pi D R_p}{\frac{2}{\mathrm{Pe}}\left[1 - \exp\left(-\frac{\mathrm{Pe}}{2}\right)\right]} \tag{11}$$

This last equation implies that, for small Peclet values, where diffusion dominates, Smoluchowski's result is retrieved ($K_{11}^S =$

$8kT/3\eta$, where η is the viscosity of the liquid and the Stokes−Einstein relation has been used), while for very large Peclet values shear-induced aggregation dominates, and the rate of aggregation is $K_{11} = 4\pi v_0(2R_p)^2 = 4\pi\dot{\gamma}(2R_p)^3$, where $\dot{\gamma}$ is the shear rate. This has the same dependence as the aggregation rate constant derived by Smoluchowski for simple shear, except that the prefactor equals 4π instead of $4/3\pi$ because of the different flow field. As expected, for the flow field used here, the rate of aggregation is larger than for any commonly encountered flow fields, and can therefore be used as an upper bound.

We have performed some calculations of aggregation rate constants using eq 10 for particles with the same surface properties as those experimentally investigated in this work. The total energy of interaction has been first calculated as the sum of the van der Waals attractive contribution and the electrostatic repulsive contribution. The van der Waals attractive contribution has been calculated using a modified Hamaker formulation reported in the literature,[36] with the Hamaker constant values for polystyrene:

$$\Phi_a = -\frac{A_H(r)}{6}\left[\frac{2R_p^2}{r^2-4R_p^2}+\frac{2R_p^2}{r^2}+\ln\left(\frac{r^2-4R_p^2}{r^2}\right)\right] \quad (12)$$

where r is the center-to-center distance between two particles and $A_H(r)$ is the usual Hamaker constant, which is a function of distance and ionic strength of the solution and accounts for retardation effects.

The electrostatic interactions are described using the equation derived by Sader, Carnie, and Chan,[35] which is highly accurate for spherical particles with high values of surface potential ψ_0:

$$\Phi_r = \frac{4\pi\varepsilon}{e_l^2}\left\{4\exp\left(\frac{\kappa(r-2R_p)}{2}\right)\tanh^{-1}\left[\exp\left(\frac{\kappa(r-2R_p)}{2}\right)\times \tanh\left(\frac{\psi_0 e_l}{kT}\right)\right]\right\}^2\frac{R_p^2}{r}\ln\{1+\exp[-\kappa(r-2R_p)]\} \quad (13)$$

where e_l is the electron charge, and κ is the Debye−Hückel parameter.

The dash-dotted line in Figure 7 shows the DLVO potential ($\Phi_{DLVO} = \Phi_a + \Phi_r$) computed using a surface potential equal to −60 mV (equal to the zeta-potential of results for fully covered C particles measured with a Zeta-Nanosizer 2000 instrument, Malvern, U.K.) and a Debye length of $1/\kappa \sim 43$ nm, since the only electrolytes present in solution are the counterions of the surface charged groups and surfactant molecules. Note that these conditions correspond to a homogeneous film of surfactant on the particles. Figure 8 shows the aggregation rate constant, K_{11}, normalized by the Smoluchowski rate constant under diffusion-limited conditions, K_{11}^S, in the case where interactions are neglected, and therefore the particles stick together upon collision as a result of the flow (dashed line, $\Phi \equiv 0$), or are accounted for (continuous line). At low Peclet numbers, the aggregation rate of the particles is negligible because the Fuchs stability ratio is $W \sim 10^{250}$, which is a typical value for large particles in solutions containing low electrolyte concentration and having high surface potential. However, one can observe that, as the Peclet number increases, i.e., as the shear rate increases, a critical value is reached (Pe ∼ 800) where the rate of aggregation increases abruptly, and eventually reaches the corresponding value obtained in the absence of interactions. This implies that, at very low concentrations of electrolytes and high surface potential, large particles subject to a high shear rate could be rapidly coagulated. In addition, above a certain shear rate the aggregation rate values are independent of the presence of a repulsive barrier. A qualitatively analogous behavior has been obtained by Melis et al.[39] for more realistic elongational flow.

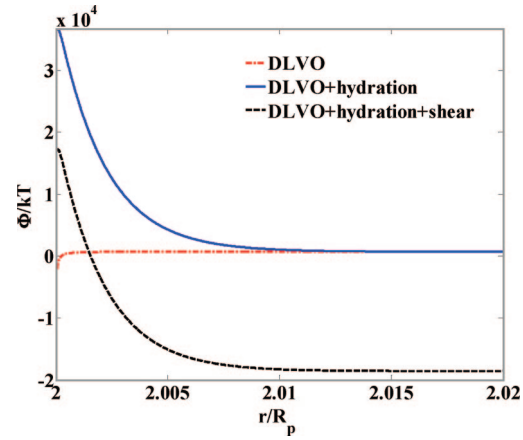

Figure 7. Interaction potential energy curves calculated based on eqs 12 and 13, showing the relative importance of the DLVO term (DLVO), of the shear-induced collision energy (shear) and of the hydration forces (hydration), plotted as a function of the center-to-center distance between the particles normalized by the radius of the particles.

On the basis of the previous discussion, it is possible to define a simple criterion to check the stability of a dispersion of charged interacting colloidal particles subject to shear flow, once the surface potential is known. From eq 10, the aggregation rate constant and the corresponding aggregation regimes depend essentially on the balance between the two terms that are summed up in the argument of the exponential at the denominator. It seems natural, thus, to define a nondimensional number M in the following way:

$$M = \frac{12\pi\eta v_0 R_p^3/r_M}{\Phi(r_M)} \quad (14)$$

with r_M being the position of the maximum in the repulsive energy barrier, i.e., the position at which $d\Phi/dr \equiv 0$. It follows that for $M \ll 1$, the dominant forces are clearly the colloidal interactions, and the Fuchs aggregation rate constant is retrieved: $K_{11} \rightarrow K_B/W$. On the other hand, when shear forces dominate over the interparticle interactions, eq 11 is obtained. It is worth pointing out that, when comparing shear energies with colloidal interaction energies, the former are present only transiently, i.e., only during the shearing process, while the colloidal interaction energies are an intrinsic property of the colloidal system and, thus, are always present, independently of the application of shear.

The above results led us to the conclusion that classical DLVO theory cannot explain the stability of the particles at high shear rates such as those experienced by the particles in the MC. According to our analysis above, in fact, even in the case of highest DLVO repulsion (particles covered by a homogeneous surfactant film), there should be an achievable value of shear collision energy capable of coagulating the particles, something that is contradicted by the experiments where we noted the impossibility of coagulating particles bearing a homogeneous surfactant film even at Pe numbers well above 800. An additional repulsive force, not included in the DLVO theory, therefore, must be responsible for that.

It is well-known that the DLVO theory at very short separations between two surfaces needs to be corrected in order

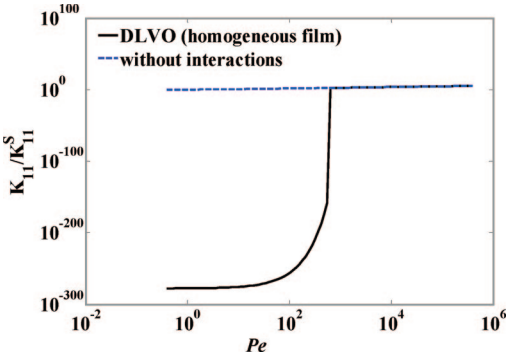

Figure 8. The aggregation rate constant K_{11} normalized by the Smoluchowski diffusion-limited value K^S_{11} plotted as a function of the Peclet number (Pe). The solid line represents the case where interactions are accounted for (eq 10), while the dashed line represents the case with no interactions (eq 11).

to account for repulsive hydration forces. Strong hydration forces have been measured between surfaces coated by dense layers of phospholipids and surfactants in the low-salt limit.[40,41] Typically, the effects of hydration forces between hydrophilic (structure-making) surfaces are very strong at very small separation distances and in the low-salt limit, but decay exponentially with the separation distance and their effect becomes negligible at a few nanometers distance:[41]

$$\Phi_{hydr} = w_0 \pi R_p \lambda \exp\left(-\frac{(r-2R_p)}{\lambda}\right) \qquad (15)$$

where λ determines the range of interaction, while w_0 determines the magnitude of the interactions. In Figure 7, a plot of the DLVO profile at short distances from the surface is shown ($\Phi = \Phi_{DLVO} = \Phi_a + \Phi_r$), together with the effect of hydration ($\Phi = \Phi_{DLVO} + \Phi_{hydr}$) and of shear forces ($\Phi = \Phi_{DLVO} + \Phi_{hydr} + \Phi_{shear}$, where $\Phi_{shear} = (12\pi\eta v_0 R_p^2/kT)(R_p/r)$), for conditions close to those experimentally obtained in the MC. For the lower limiting boundary of the hydration interaction energy, we have used the following parameters: $w_0 = 0.3$ J/m^2 and $\lambda = 6$ Å. One can see that, with the hydration forces, the primary minimum is completely eliminated, thus preventing the occurrence of aggregation. In addition, while it is clear that DLVO interactions cannot compete alone with shear forces, (which are almost 1 order of magnitude larger than the barrier), the presence of the hydration forces is sufficient to provide additional stability to the particles. We can therefore conclude that, under low electrolyte concentrations, the structure of the surfactant layer completely covering the particles generates strong hydration forces that are able to prevent shear-induced aggregation. When comparing the w_0 and λ values applied here with values in the literature, we can see that, while λ is not far from typical values of $\lambda \approx 3$ Å, w_0 is 1 order of magnitude larger than the typical values reported by Israelachvili,[41] who gives, as an upper bound, $w_0 = 0.03$ J/m^2. However, using the interaction constant calculated by Faraudo and Bresme[42] for simulations of interactions between sodium dodecyl sulfate (SDS) layers in the presence of only the surfactant counterions, we would have $w_0 \sim 10^3$ J/m^2. It is possible, then, that our value is larger than the typical values measured for systems with added electrolyte[41] because the anomalous dielectric response of water at small interparticle distances (which is believed to be responsible for the hydration forces) is different depending on the presence or absence of added electrolyte. This sounds reasonable if one considers that the organization of water molecules might become more structured in the absence of added electrolyte, thus leading to enhanced repulsion.

IV. Conclusions

The presence of a film of charged amphiphilic molecules on the surface of Brownian particles can influence their mutual interaction as well as their interaction with other surfaces. It is therefore important to quantify and understand the interactions in relation to the physical properties, structure, and phases of the film. The latter aspects have been investigated by analyzing the adsorption isotherms of different ionic amphiphilic molecules on polymer submicron particles. A gas-like phase (noninteracting molecules) is followed, with increasing concentration, by the appearance of condensed patches of molecules coexisting with the gas-like phase. Saturation of the surface sets in when the condensed phase occupies the entire surface of the particles. By imparting high collision-energy to the particles in a high-shear MC with no added salts, we have demonstrated that the interaction is less repulsive as long as gaseous or molecule-free domains are present. On the other hand, if the particles are entirely covered by a fully developed monolayer, aggregation is unachievable, despite the very high collision energy, thus revealing a very high repulsive barrier. To explain the nature of the latter, we propose a simple model based on the diffusion−convection equation, which provides a criterion to know the stability of a colloidal dispersion under shear in the low-salt limit. On the basis of this model, we show the importance of hydration forces in making the aggregation of such particles impossible in the low-salt regime. A reasonable lower limiting boundary for the hydration interaction potential energy is calculated and compared with data in the literature.

All these findings show strong analogies with the scenario depicted by Israelachvili and co-workers,[43] who found that, in the case of lipid and surfactant bilayers in aqueous solution, adhesion and fusion are possible, provided that either salt is added to system (allowing for adhesion) or the molecular layers are not fully developed ("empty" patches are then present, interacting attractively via hydrophobic interaction), leading to fusion of the bilayers. However, in the systems investigated by these authors, adhesion is also never possible for fully developed layers in the low-salt limit due to hydration forces. On the basis of the present work, this knowledge can now be extended from the well-studied case of macroscopic surfaces to the case of Brownian particles.

Acknowledgment. Financial support of BASF AG (Ludwigshafen, Germany) and the Swiss National Science Foundation (Grant No. 200020-113805/1) is gratefully acknowledged.

References and Notes

(1) Castelvetro, V.; De Vita, C. *Adv. Colloid Interface Sci.* **2004**, *108* (109), 167.
(2) Rosen, H.; Abribat, T. *Nat. Rev. Drug Discovery* **2005**, *4*, 381.
(3) Date, A. A.; Joshi, M. D.; Patravale, V. B. *Adv. Drug Delivery Rev.* **2007**, *59*, 505.
(4) Lynch, I.; Cedervall, T.; Lundqvist, M.; Cabaleiro-Lago, C.; Linse, S.; Dawson, K. A. *Adv. Colloid Interface Sci.* **2007**, *134*, 167.
(5) Turner, S. F.; Clarke, S. M.; Rennie, A. R.; Thirtle, P. N.; Cooke, D. J.; Li, Z. X.; Thomas, R. K. *Langmuir* **1999**, *15*, 1017.
(6) Bremmell, K. E.; Kingshott, P.; Ademovic, Z.; Winther-Jensen, B.; Griesser, H. J. *Langmuir* **2006**, *22*, 313.
(7) Alig, A. R. G.; Gourdon, D.; Israelachvili, J. *J. Phys. Chem. B* **2007**, *111*, 9.
(8) Manne, S.; Gaub, H. E. *Science* **1995**, *270*, 1480.
(9) Schniepp, H. C.; Shum, H. C.; Saville, D. A.; Aksay, I. A. *J. Phys. Chem. B* **2007**, *111*, 8708.
(10) Lee, W. P.; Gundabala, V. R.; Akpa, B. S.; Johns, M. L.; Jeynes, C.; Routh, A. F. *Langmuir* **2006**, *22*, 5314.

(11) Kawasaki, H.; Ban, K.; Maeda, H. *J. Phys. Chem. B* **2004**, *108*, 16746.
(12) Drelich, J.; Long, J.; Xu, Z.; Masliyah, J.; White, C. L. *J. Colloid Interface Sci.* **2006**, *303*, 627.
(13) Grillo, I.; Levitz, P.; Zemb, T. *Eur. Phys. J. B* **1999**, *10*, 29.
(14) Oberdisse, J. *Curr. Opin. Colloid Interface Sci.* **2007**, *12*, 3.
(15) Wu, C. *Macromolecules* **1994**, *27*, 7099.
(16) Wu, C. *Macromolecules* **1994**, *27*, 298.
(17) Cummins, P. G.; Staples, E.; Penfold, J. *J. Phys. Chem.* **1990**, *94*, 3740.
(18) Brown, W.; Zhao, J. X. *Macromolecules* **1993**, *26*, 2711.
(19) Zaccone, A.; Wu, H.; Lattuada, M.; Morbidelli, M. *J. Phys. Chem. B* **2008**, *112*, 1976.
(20) Zhu, B. Y.; Gu, T. R. *J. Chem. Soc., Faraday Trans. 1* **1989**, *85*, 3813.
(21) Zhu, B. Y.; Gu, T. R. *J. Chem. Soc., Faraday Trans. 1* **1991**, *87*, 2745.
(22) Peierls, R. E. *Ann. Inst. Henri Poincaré* **1935**, *5*, 1771.
(23) Landau, L. D. *Phys. Z. Sowjetunion* **1937**, *11*, 26.
(24) Landau, L. D.; Lifshitz, E. M. *Statistical Physics*; Pergamon: Oxford, 1958.
(25) Dash, J. G. *Films on Solid Surfaces*; Academic Press: New York, 1975.
(26) Torquato, S.; Truskett, T. M.; Debenedetti, P. G. *Phys. Rev. Lett.* **2000**, *84*, 2064.
(27) Wu, H.; Lattuada, M.; Sandkuhler, P.; Sefcik, J.; Morbidelli, M. *Langmuir* **2003**, *19*, 10710.
(28) Zhu, B. Y.; Gu, T. R. *Adv. Colloid Interface Sci.* **1991**, *37*, 1.
(29) Whitesides, G. M.; Mathias, J. P.; Seto, C. T. *Science* **1991**, *254*, 1312.
(30) Piirma, I.; Chen, S. R. *J. Colloid Interface Sci.* **1980**, *74*, 90.
(31) Vincent, J. M.; Skoulios, A. *Acta Crystallogr.* **1966**, *20*, 432.
(32) Adamson, A. W. *Physical Chemistry of Surfaces*; John Wiley & Sons: New York, 1976.
(33) Zhang, R.; Somasundaran, P. *Adv. Colloid Interface Sci.* **2006**, *123*, 213.
(34) Russel, W. B.; Saville, D. A.; Schowalter, W. R. *Colloidal Dispersions*; Cambridge University Press: Cambridge, 1989.
(35) Sader, J. E.; Carnie, S. L.; Chan, D. Y. C. *J. Colloid Interface Sci.* **1995**, *171*, 46.
(36) Vanni, M.; Baldi, G. *Adv. Colloid Interface Sci.* **2002**, *97*, 151.
(37) Fuchs, N. *Z. Phys.* **1934**, *89*, 736.
(38) von Smoluchowski, M. *Z. Phys. Chem.* **1917**, *92*, 129.
(39) Melis, S.; Verduyn, M.; Storti, G.; Morbidelli, M.; Baldyga, J. *AIChE J.* **1999**, *45*, 13.
(40) Cowley, A. C.; Fuller, N. L.; Rand, R. P.; Parsegian, V. A. *Biochemistry* **1978**, *17*, 3163.
(41) Israelachvili, J. *Intermolecular and Surface Forces*; Academic Press: San Diego, 1992; Chapter 18.
(42) Faraudo, J.; Bresme, F. *Phys. Rev. Lett.* **2005**, 94.
(43) Helm, C. A.; Israelachvili, J. N.; McGuiggan, P. M. *Science* **1989**, *246*, 919.

JP801423H